JOURNAL OF VACUUM SCIENCE AND TECHNOLOGY A

Floating potential measurements in the near field of an ion cyclotron resonance heating antenna

J. B. O. Caughman, D. N. Ruzic, and D. J. Hoffman

Citation: J. Vac. Sci. Technol. A **7**, 1092 (1989); doi: 10.1116/1.576236

View online: http://dx.doi.org/10.1116/1.576236

View Table of Contents: http://avspublications.org/resource/1/JVTAD6/v7/i3

Published by the AVS: Science & Technology of Materials, Interfaces, and Processing

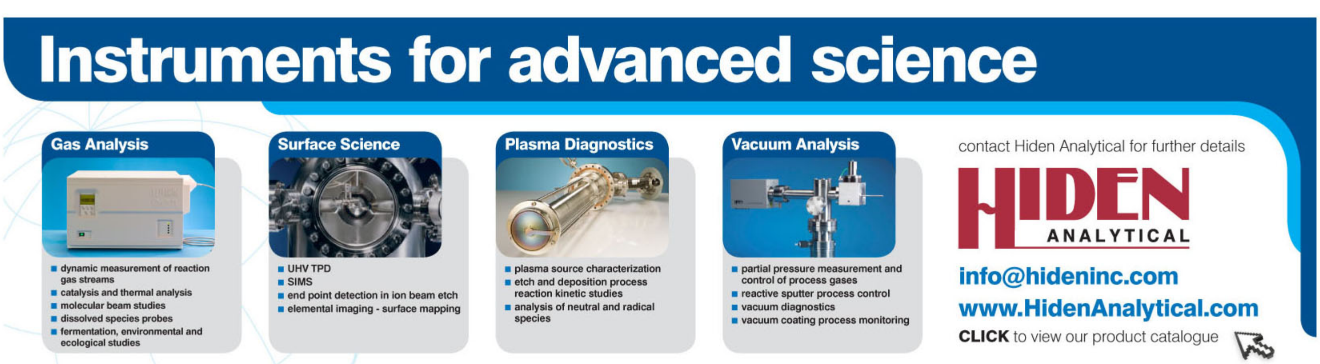

Floating potential measurements in the near field of an ion cyclotron resonance heating antenna

J. B. O. Caughman, II and D. N. Ruzic
Department of Nuclear Engineering, University of Illinois, Urbana, Illinois 61801
D. J. Hoffman
Oak Ridge National Laboratory, Oak Ridge, Tennessee 37831

(Received 7 October 1988; accepted 21 November 1988)

Large variations in the plasma potential can lead to large sheath potentials at the surface of the Faraday shield of an ion cyclotron resonance heating (ICRH) antenna. This sheath can accelerate ions to energies where sputtering is significant, resulting in impurity generation. The time-varying floating potential is being measured in the near field of an ICRH antenna by using the Radio Frequency Test Facility (RFTF) at Oak Ridge National Laboratory. The antenna used is a resonant loop antenna that has a two-tier Faraday shield with a layer of graphite on the outer tier. The electron cyclotron heated plasma in RFTF is produced by a 10.6-GHz klystron. The magnetic field at the antenna is ~ 2 kG, with a plasma density of $\sim 10^{10}$ cm^{-3} with an electron temperature of ~ 6 eV. Ionization by rf power from the antenna produces a local plasma of $\sim 10^{11}$ with an electron temperature of 12 to 20 eV. The rf floating potential is measured by using a capacitively coupled probe that is scanned in front of the antenna, parallel to the current strap. A stationary Langmuir probe is used to measure the time-averaged floating potential. Measurements indicate that the potential scales with the antenna current and increases with plasma density to values of up to 300 V peak-to-peak. The rf component of the floating potential seems to follow the near field pattern of the antenna, indicating that these fields may be responsible for the potential formation.

I. INTRODUCTION

Impurity generation and control is an important aspect of fusion research, especially in experiments involving high-power Ion Cyclotron Resonance Heating (ICRH). Experiments on several fusion machines have shown an increase in the impurity concentration during ICRH. The rf affects the transport in the edge region and generally increases the edge ion density and electron temperature.[1–3] In addition to increasing the impurity generation from the wall and limiter, the generation of impurities specifically from the Faraday shield of an ICRH antenna is a problem seen in several experiments.[2,4–7]

Experiments on the Axially Symmetric Divertor Experiment (ASDEX) have shown that the Faraday shield is a local source of impurity generation during ICRH. It was concluded that the increase in the impurity concentration is due to a change in the transport in the scrape off layer (SOL) because of radial electric fields, and the increase in the local impurity production is due to large electric fields in the area of the antenna.[6] Analysis of Faraday shields after ICRH operation have shown evidence that there is a special ion accelerating process caused by ICRH in front of the active antenna area.[8]

Experiments on the Joint European Torus (JET) have also shown that the Faraday shield is a local impurity source and that metal release from the Faraday shield is only noticeable when the antenna is activated. Experiments with adjacent antennas have shown that there is no substantial metal influx from the unpowered antenna, even when the adjacent antenna is run at high power. It was concluded that the increase in metal influx from the antenna is not caused by the increase in the parallel energy flux during ICRH, but is due to a local effect related to the rf field from the antenna.[2]

The role of the plasma sheath in the near field of an ICRH antenna is important in understanding the generation of impurities from the Faraday shield and also in modeling its effect on the plasma.[9] An experiment is being conducted to study this sheath by directly measuring the rf floating potential in the near field of an ICRH antenna by using the Radio Frequency Test Facility (RFTF) at Oak Ridge National Laboratory. The presence of a large plasma potential at the antenna can cause ions to gain a significant amount of energy as they fall through the sheath. If the sheath potential is large enough, the ion energies can approach the level where the sputtering yield is at a maximum for light ion sputtering of Faraday shield materials (500–1500 eV) and is near unity for the self-sputtering of these materials.

II. EXPERIMENT

The experiments are being conducted using RFTF with a resonant loop antenna.[10] This antenna is the same type used in D-IIID and is similar to the resonant double loop used in the Tokamak Fusion Test Reactor (TFTR) and Tore Supra, in that it is a resonant structure using a variable tuning capacitor. The antenna is shown in Fig. 1 and consists of a current strap 15.2 cm wide and 42.2 cm high that is shorted at one end and has a high-voltage variable capacitor at the other end. The current feed is located 12.1 cm from the shorted end of the current strap. The antenna is operated at 41 MHz with powers up to 60 kW. It uses a two-tier Faraday shield with a layer of graphite brazed onto the outer tier, facing the plasma.

The plasma is produced by a 10.6-GHz klystron microwave source and has a central electron density of $\sim 10^{11}$

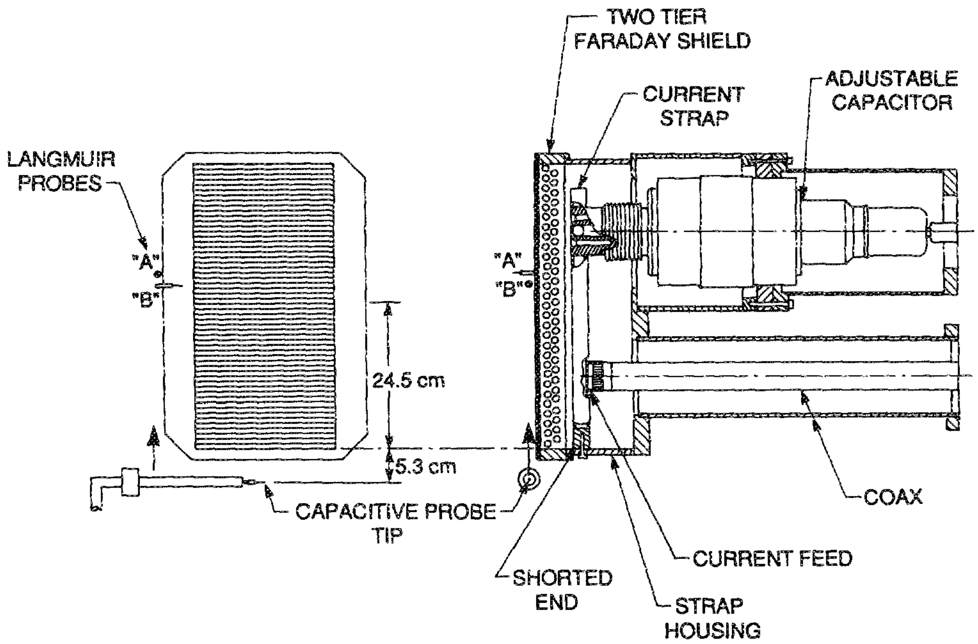

FIG. 1. Front view and sectional view of the resonant loop antenna used in the experiment showing the probe locations. The capacitive probe is scanned a total of 29.8 cm, starting 5.3 cm below the shorted end of the antenna.

cm^{-3} and an electron temperature of ~ 6 eV. The magnetic field in the area of the antenna is ~ 0.2 T. The plasma density in front of the antenna is $\sim 10^{10}\ \mathrm{cm}^{-3}$ with an electron temperature of ~ 6 eV. When the antenna is activated, ionization caused by rf power from the antenna produces a local plasma with a density of $(1–2)\times 10^{11}\ \mathrm{cm}^{-3}$ and an electron temperature of 12 to 20 eV.

The plasma is pulsed for 80 ms every 20 s, with the rf pulsed for 40 ms in the middle of the plasma pulse. The power at the rf transmitter and the voltage standing-wave ratio (VSWR) at the antenna are measured using directional couplers. From this information, the antenna load resistance, the antenna current, and the peak voltage of the antenna (at the capacitor) can be calculated using the following equations:

$$R_{\mathrm{load}} = \frac{\alpha^2(\omega L)^2}{Z_{\mathrm{in}}}\ \ \Omega, \tag{1}$$

$$I_{\mathrm{ant}} = \sqrt{\left(\frac{P_{\mathrm{rf}}}{R_{\mathrm{load}}}\right)}\ \ \mathrm{A(rms)}, \tag{2}$$

$$|V_{\mathrm{cap}}| = I_{\mathrm{peak}}|Z_{\mathrm{cap}}| = \frac{\sqrt{2}I_{\mathrm{ant}}}{\omega C}\ \ \mathrm{V(peak)}, \tag{3}$$

where P_{rf} is the rf power, $Z_{in} = 50(\mathrm{VSWR})$, $1/\omega C = \omega L$ (at resonance), L is the inductance of the current strap, and α is the fraction of L appearing between the current feed and the shorted end.

The rf floating potential is measured with a capacitive probe that is scanned in front of the antenna, parallel to the current strap, from 5.3 cm below the shorted end of the antenna to 24.5 cm above the shorted end (see Fig. 1). The probe tip is ~ 2 mm from the Faraday shield surface and is in line with the center of the current strap, at the position where the magnetic field is parallel to the shield surface. The capacitive probe consists of 0.38-mm-diam tungsten wire enclosed in ceramic tubing at the tip and sealed with ceramic cement. The probe tip is 4 mm long and 1.2 mm in diam and has a capacitance of ~ 0.5 pF. The probe tip acts as a coaxial capacitor, with the wire acting as the inner electrode, the plasma acting as the outer electrode, and the ceramic tubing acting as the dielectric.[11] The plasma sheath can also act as an additional tip capacitance and will be discussed in Sec. IV.

The capacitively coupled signal is shunted across a capacitance to ground and fed into a high-input impedance buffer circuit shown in Fig. 2. The shunt capacitance consists of the capacitance between the wire and the shield of the probe body, and a capacitor added to the circuit. The buffer circuit consists of a junction-FET and a NPN transistor connected to 50-Ω coax cable terminated on 50 Ω.[11] This circuit has almost constant gain for frequencies up to 65 MHz. The probe circuit is contained inside a $\frac{3}{4}$-in.-o.d. stainless-steel tube and is within 12 cm of the probe tip. The circuit has to be as close to the probe tip as possible to decrease any standing-wave effects because the probe body acts as a transmission line that is not terminated on its characteristic impedance.[12] The probe is calibrated by inserting the probe tip into a cup of mercury that has a known potential applied to it.[11]

The rf floating potential in front of the antenna is mea-

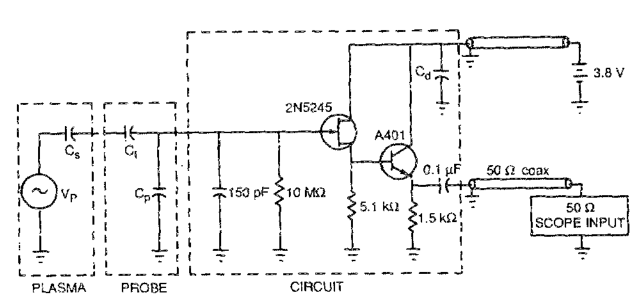

FIG. 2. Schematic of the capacitive probe circuit. C_s is the sheath capacitance, C_t is the capacitance of the probe tip (0.5 pF), C_p is the capacitance of the probe body between the inner wire and the shield (30 pF), and C_d is a 0.1-μF capacitor to decouple the power line.

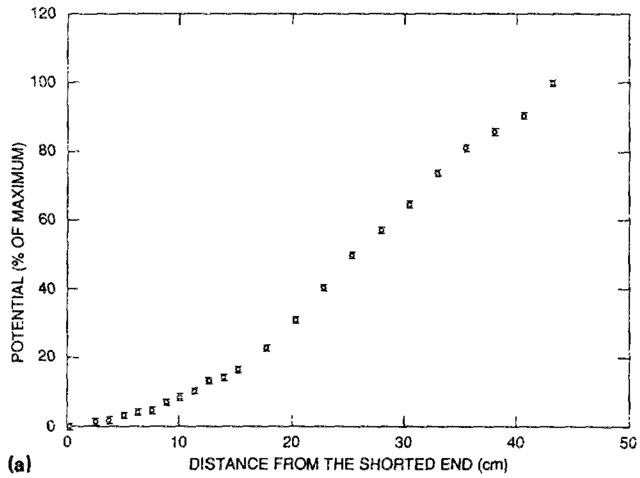

(a)

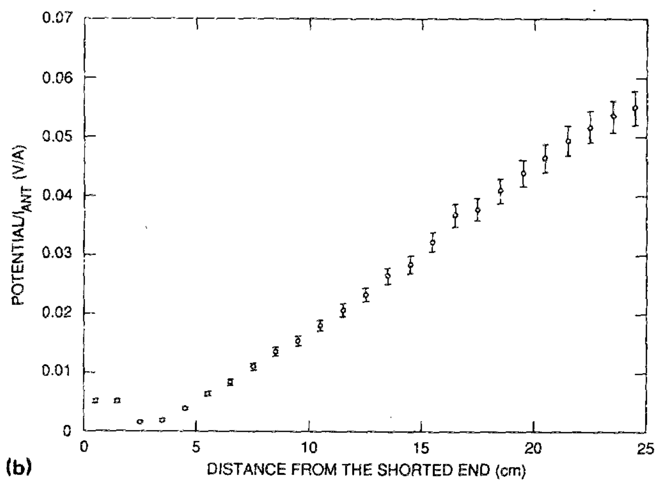

(b)

FIG. 3. (a) Voltage distribution on the current strap of the antenna without the Faraday shield. The voltage goes from a minimum at the shorted end to a maximum at the capacitor end. The capacitor voltages ranged from 7 to 20 kV. (b) Potential measured with the capacitive probe in air. The potential follows a similar pattern as the voltage on the current strap.

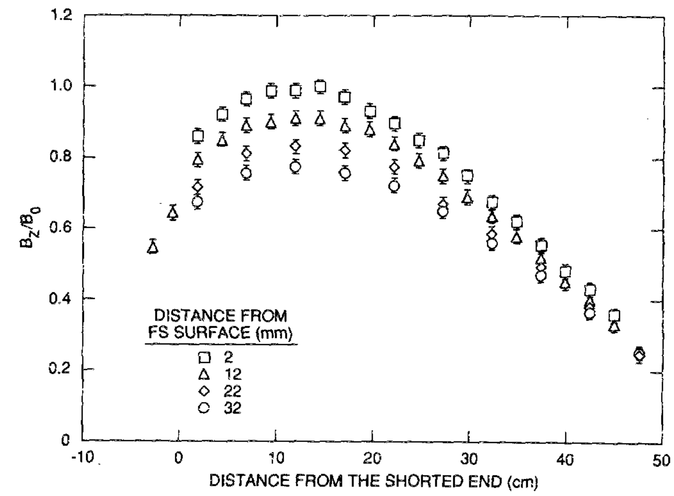

FIG. 4. Antenna magnetic field pattern in the z direction (toroidal) measured with a magnetic loop probe at several positions moving away from Faraday shield surface. The antenna is operated at 41 MHz, and the data are normalized by the peak field measured 2 mm from the shield surface.

sured for a variety of rf powers and gas pressures. At each point where the potential is measured, the transmitter power and antenna VSWR are measured, and the peak antenna voltage, the antenna load resistance, and the antenna current are calculated. The potential measured by the probe is then normalized by the antenna current so that comparisons between different rf powers and gas pressures can be made for the same relative antenna rf field conditions.

In addition to the capacitive probe, two stationary Langmuir probes are used to measure the plasma characteristics near the antenna. The probes are located 27 cm from the shorted end of the antenna, with one parallel to the Faraday shield surface (probe B) and one perpendicular to the shield surface (probe A) in a position that intersects a magnetic field line that just grazes the shield surface (see Fig. 1). These probes are terminated on low impedances so that the "ac" and "dc" load lines are near vertical, allowing more accurate current readings as the probe bias voltage is changed.[13,14]

III. RESULTS

The voltage distribution on the current strap of the antenna without the Faraday shield, measured with a vector voltmeter, is shown in Fig. 3(a). As expected, the voltage is approximately linear, going from a minimum at the shorted end to a maximum at the capacitor. The capacitor voltages ranged from 6.87 ± 0.38 kV at a rf power of 10.1 ± 1.0 kW to 18.33 ± 1.0 kV at a rf power of 64.7 ± 6.5 kW. The potential measured by the capacitive probe in front of the antenna with the Faraday shield follows the same type of pattern when measured in air and is shown in Fig. 3(b). This measurement indicates that the probe is coupling electrostatically to potential (on the current strap) and not coupling to electromagnetic pickup. Another indication that the probe is coupling electrostatically to potential is that the probe signal drops dramatically when the probe tip is aligned with a Faraday shield tube and has no direct line of sight with the current strap. The rf magnetic field pattern of the antenna, measured with a magnetic loop probe in air without the external magnetic field, is shown in Fig. 4.

The antenna load resistance is shown in Table I for several gas pressures and rf powers. At low rf powers ($\leqslant 15$ kW), the load resistance generally increases with gas pressure and seems to saturate as the rf power is increased.

The plasma induced noise on the Langmuir probe signals makes it difficult to measure the density and temperature accurately. The general trend shows that the ion saturation

TABLE I. Antenna load resistance for different gas pressures and rf powers.

Gas pressure (mTorr)	rf power (kW)	Antenna load resistance (mΩ)
0.1	13.7 ± 1.4	176 ± 9
	25.4 ± 2.5	169 ± 10
0.2	10.1 ± 1.0	265 ± 16
	22.6 ± 2.3	335 ± 24
	33.3 ± 3.3	300 ± 19
0.3	11.6 ± 1.2	319 ± 14
	32.8 ± 3.3	230 ± 19
	54.3 ± 5.4	222 ± 14

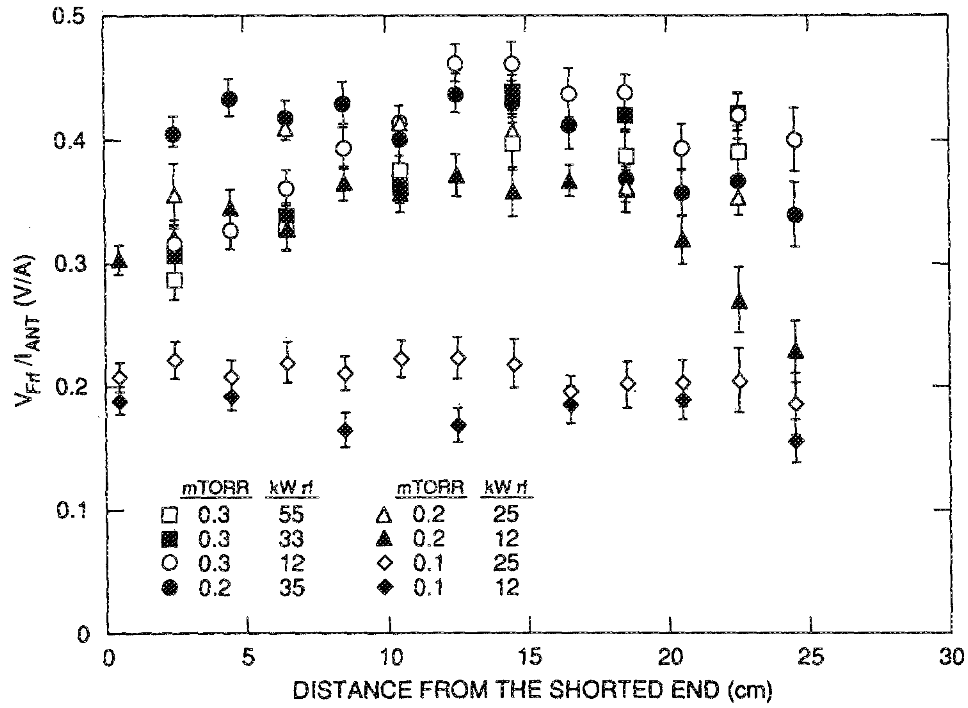

FIG. 5. rf floating potential, normalized by the antenna current, measured with the capacitive probe 2 mm from the Faraday shield surface. The potentials follow the field pattern much more closely than they follow the voltage distribution on the current strap, indicating that the antenna near fields may be responsible for the potential formation.

current, measured with a high negative bias on the probes, increased with gas pressure and rf power. Also, the rf potential measured with the capacitive probe generally increases when the ion saturation current increases, indicating that there may be a density dependence on the rf component of the plasma potential. The electron temperature measured with the Langmuir probes is 14–19 eV on probe A and 12–14 eV on probe B. The temperature dependence on gas pressure and rf power is not discernible from the data, due to the uncertainties in the measurements. The density ranged from 1.5 to 2×10^{10} cm^{-3} at 0.1 mTorr, 3 to 5×10^{10} cm^{-3} at 0.2 mTorr, and 5 to 20×10^{10} cm^{-3} at 0.3 mTorr.

The rf floating potential, normalized by the antenna current, is shown in Fig. 5 for gas pressures of 0.1, 0.2, and 0.3 mTorr for the rf powers indicated. The error bars are from the error involved in calculating the VSWR used in the antenna current calculation and from the amount of uncertainty in the capacitive probe measurement. The data show the trend of being fairly level in the middle and falling slightly at the ends. The normalized rf potentials are lower for the 0.1 mTorr pressure and about the same for the 0.2 and 0.3 mTorr pressures, with the low-power rf experiment at 0.2 mTorr being slightly lower. These potentials follow the field pattern much more closely than they follow the voltage distribution on the current strap, indicating that the near fields of the antenna may be responsible for this potential formation. The potentials ranged from 58 ± 3 V (peak) for an antenna current of 280 ± 16 A and rf power of 13.7 ± 1.4 kW at 0.1 mTorr pressure to 150 ± 5 V (peak) for an antenna current of 411 ± 25 A and rf power of 50.7 ± 5.0 kW at 0.3 mTorr pressure.

The dc floating potential V_F of the plasma is measured using the Langmuir probe that intersects the flux tube that just grazes the Faraday shield surface (probe A). The floating potential is measured by changing the bias voltage until the total current measured by the probe is zero. For this set of experimental data, the probe is terminated on small impedances that have almost vertical load lines for both the ac and dc components of the probe characteristic. This method gives good measurements of time averaged probe current in the presence of rf. However, the floating potential from the time-averaged current will be lower than the time-averaged floating potential, due to sheath rectification by the rf at the probe tip. This sheath rectification causes a negative self-bias to develop. If the plasma potential varies sinusoidally and the electron temperature is not varying with time, the self-bias voltage can be expressed as[14,15]

$$V_{SB} = -\left(\frac{T_e}{e}\right)\ln[I_0(e\tilde{V}/T_e)]\,, \tag{4}$$

where $\tilde{V}$ is the magnitude of the rf part of the potential and I_0 is the zeroth order modified Bessel function of the argument $e\tilde{V}/T_e$. This value of self-bias voltage is then used to correct the floating potential from the current measurement to approximate the time-averaged floating potential. For most cases, this correction term is <30 V.

The time-averaged floating potential (corrected for self-bias) is shown in Table II for several gas pressures and antenna currents. At 0.2 and 0.3 mTorr, the ratio of V_F/I_{ant} is the same (within the error bars) for the two antenna currents shown, and is about the same as the ratio for the rf component shown in Fig. 5. These results indicate that the dc component of the floating potential follows the same type of scaling as the rf component at these pressures and power levels, and has a floating potential with a rf magnitude that is about equal to the dc magnitude. At 0.1 mTorr, V_F/I_{ant} is the same as in the other cases for the lower antenna current, but decreases with higher antenna current. These results indicate that the floating potential has a rf magnitude that is smaller than the dc magnitude as the antenna current is increased.

The floating potential measured with the Langmuir probe

TABLE II. Time-averaged floating potential (corrected for self-bias) for different gas pressures and antenna currents. These results are from the probe that intersects the field line that grazes the Faraday shield surface (probe A).

Gas pressure (mTorr)	V_F (V)	I_{ant} (A)	V_F/I_{ant} (V/A)
0.1	101 ± 7	235 ± 15	0.430 ± 0.038
	146 ± 7	403 ± 25	0.362 ± 0.028
	177 ± 8	574 ± 33	0.308 ± 0.024
	204 ± 9	701 ± 41	0.291 ± 0.023
0.2	95 ± 7	208 ± 12	0.457 ± 0.038
	122 ± 9	275 ± 16	0.444 ± 0.038
0.3	64 ± 8	162 ± 10	0.395 ± 0.055
	132 ± 9	315 ± 21	0.419 ± 0.040

parallel to the Faraday shield surface (probe B) is smaller than that measured on the probe intersecting the grazing field line (probe A). For example, the time-averaged floating potential (corrected) at 0.1 mTorr is 156 ± 8 V for an antenna current of 701 ± 41 A and at 0.2 mTorr is 75 ± 7 V for an antenna current of 208 ± 12 A. In general, the ion saturation current is $\sim 50\%$ lower on probe B than it is on probe A and the electron temperature is $\sim 20\%$ lower, indicating lower plasma density. The lower plasma density at probe B along with the lower floating potential is another indication that there may be a density dependence on the plasma potential change due to rf.

The waveform of the floating potential is shown in Fig. 6(a). It consists of a dc component and an ac component. The ac component is the rf part of the potential and is measured with the capacitive probe. The waveform from the probe appears to be sinusoidal for all the powers and pressures investigated thus far. The dc component is equivalent to the time-averaged value of the floating potential and is measured with the Langmuir probes. The potential shown is for an antenna current of 275 A at a gas pressure of 0.2 mTorr using the scaling shown in Fig. 5 for the rf component and the measured value of the dc component.

IV. DISCUSSION

The neutral density and the fractional ionization at the antenna in RFTF are different than in a tokamak edge environment. The neutral density at the antenna is higher, although some plasma configurations in tokamaks have shown a neutral pressure of up to 1 mTorr[16] (compared to 0.1–0.3 mTorr in RFTF). The plasma density for the experiments range from 0.2 to 2×10^{11} cm^{-3} compared to densities of $(1\text{–}5) \times 10^{12}$ cm^{-3} at the antenna in tokamaks.[2,17] The fractional ionization at the antenna ranges from 0.5% to 2% for the experiments, which is lower than for a tokamak. For example, the fractional ionization at the limiter in Princeton Large Torus (PLT) was 80%–90%.[18] The rf potentials measured generally increase as the fractional ionization increases, indicating that the rf potentials increase with the plasma density. These results indicate that the potentials may be significant at an ICRH antenna in a tokamak edge environment, because of the increased fractional ionization

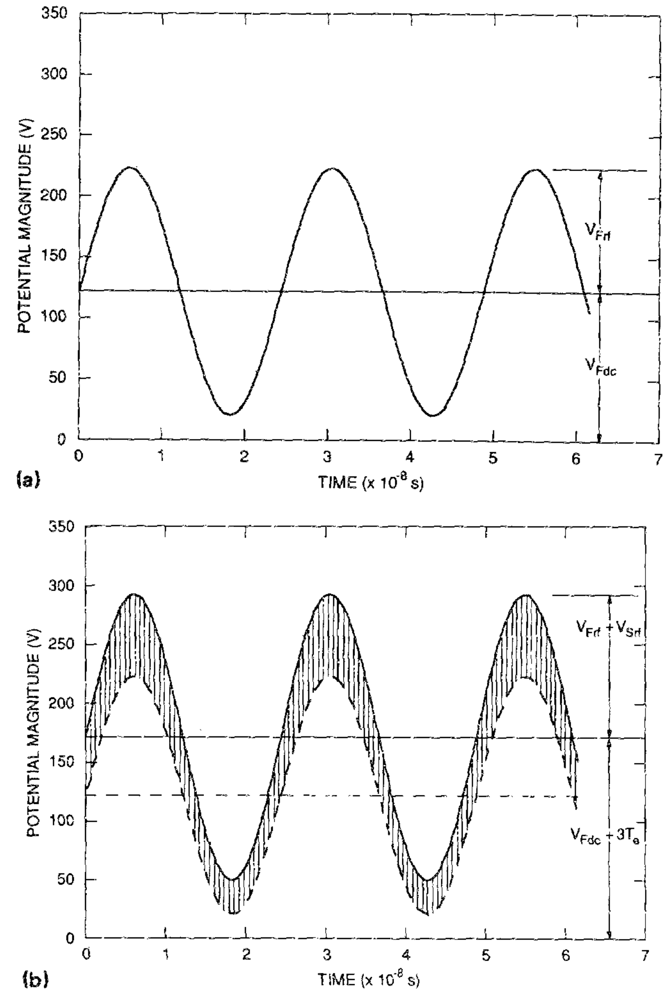

FIG. 6. (a) Waveform of the floating potential showing the ac potential measured with capacitive probe and the dc potential measured with the Langmuir probe. The case shown is for an antenna current of 275 A. (b) Waveform of the plasma potential showing the upper and lower bounds. The dc value of the plasma potential is $\sim 3T_e$ higher than the dc floating potential and the ac value of the plasma potential is probably $< 20\%$ higher than the ac floating potential.

and increased plasma density in a tokamak. The effect of lower plasma density on the rf component of the potential can be seen in Fig. 5. The plasma density and the antenna load resistance are lower for the experiment at 0.1 mTorr. Hence, the antenna current is larger and the normalized rf potential is smaller. Future experiments will include scanning a Langmuir probe in the same area as the capacitive probe to study any potential dependence on the local plasma density.

The potentials measured by this experiment are the floating potentials and not the plasma potentials. However, the two are related by the equation[19]

$$V_P = V_F + V_{SRF} + \frac{1}{2}\frac{kT_e}{e} + \frac{kT_e}{2e}\ln\left(\frac{M_i(1-\gamma)^2}{2\pi m_e(1+T_i/T_e)}\right) \quad (5)$$

which assumes a presheath potential of 0.5 kT_e/e and no fluctuations in the electron temperature. V_{srf} is the rf potential drop across the sheath due to the capacitance of the sheath, V_F is the floating potential, consisting of a dc component and an ac component described previously, and γ is the secondary electron emission coefficient. The measured floating potentials will be closer to the plasma potential if there is significant secondary electron emission from the probe tips.[20] High-energy electrons from the tail of the electron distribution caused by the microwave produced plasma in RFTF can get through the sheath at the probe tips and cause secondary electron emission.

Another factor that may affect the rf potential measurement is the capacitance of the rf sheath at the probe tip. This capacitance can act as a series capacitor between the plasma and the probe tip and makes the effective capacitance of the probe tip smaller, causing a smaller coupled signal to the probe. This effect becomes less important at higher densities because the sheath thickness is smaller.[21,22] The higher density decreases the sheath capacitance and causes the measured potential to be closer to the plasma potential.

The rf potentials measured at the lower gas pressures are smaller than those measured at the higher gas pressures. Since the density is lower for the experiments at 0.1 mTorr (as indicated by the ion saturation current), the effect of the sheath capacitance on the probe measurement will be greater. This effect can be tested by using two capacitive probes with different tip capacitances but the same physical size.[11] The measured signals will be different by the difference in the effective tip capacitances. Since the tip capacitance of each probe is known (from the calibration), the average sheath capacitance can be measured and used as a correction factor. Experiments using this two-probe method in a rf plasma discharge at the University of Illinois, with a lower plasma density than in RFTF, show that neglecting the effects of the sheath results in measured rf floating potentials that are too low by $<20\%$.[23]

The waveform of the plasma potential is shown in Fig. 6(b). From Eq. (5), the dc plasma potential will be higher than the floating potential by $\sim 3.0T_e$ and the rf plasma potential will be higher by the potential drop due to the sheath capacitance. Due to the uncertainties in the effect of secondary electron emission at the probe tips and the magnitude of the sheath capacitance, the measured potentials can be interpreted as a lower bound of the plasma potential with Eq. (5) acting as the upper bound. The true plasma potential will be between these values and is signified by the shaded area in the figure.

The potentials measured for the conditions in RFTF will cause ions hitting the Faraday shield to gain a significant amount of energy as they fall through the sheath. Since the Faraday shield is well grounded, the ions hitting the surface will have energies that can be as high as the sum of the magnitudes of the rf and dc plasma potentials.[24] Also, the magnetic field will increase the incident angle (measured from the surface normal) of the ions. Recent studies[21,22] suggest that the average impact angle increases as the magnetic field gets closer to being parallel with a surface, as is the situation with an ICRH antenna in a fusion device.

Without the rf, the sheath potential at the Faraday shield is 3–4 times the electron temperature, which is typically 10–20 eV at the antenna.[2] An ion will gain no more than 80 eV from this sheath. With the rf, however, the ions will gain a significant amount of energy from the rf plasma sheath at the Faraday shield surface. As an example, from the measured results from Fig. 5, an ion hitting the surface will have an energy of 360 to 420 eV at the average sheath potential and 720 to 780 eV at the maximum sheath potential, for an antenna current of 900 A. This energy is near the peak sputtering yield (within a factor of 2) for deuterium sputtering of carbon, nickel, beryllium, and TiC, and has a sputtering yield close to unity for self-sputtering of carbon and nickel. An ion with a grazing incidence in this energy range will cause these yields to increase further.[25]

V. CONCLUSIONS

These experiments have shown that large plasma potentials do exist in front of an ICRH antenna. The magnetized rf sheath resulting from these large potentials will cause ions to gain significantly more energy than they would without the rf effects. The energy that they gain can be near the maximum sputtering yield for many Faraday shield materials and can cause an increase in the impurity generation. The rf component of the potential seems to follow the near field pattern of the antenna, indicating that these fields may be responsible for the potential formation. Results also indicate that there may be a density dependence on the magnitude of the rf component of the potential. Future experiments will include measuring the ion energies hitting the Faraday shield using a small gridded energy analyzer and measuring local plasma density and electron temperature by scanning a Langmuir probe in the same area as the capacitive probe.

ACKNOWLEDGMENTS

This research was supported by the Magnetic Fusion Energy Technology Fellowship Program administered by Oak Ridge Associated Universities for the U.S. Department of Energy, the U.S. DOE Contract No. DE-AC05-840R21400 and Subcontract No. 19X-SB359V with Martin Marietta Energy Systems, Inc., and by the NSF Presidential Young Investigators Award NSF-CBT-84-51599.

[1] S. A. Cohen, S. Bernabei, R. Bundy, T. K. Chu, P. Colestock, E. Hinnov, W. Hooke, J. Hosea, D. Hwang, F. Jobes, D. Manos, R. Motley, D. Ruzic, J. Stevens, B. Stratton, S. Suckewer, S. Von Goeler, and R. Wilson, J. Nucl. Mater. **128/129**, 280 (1984).

[2] M. Bureš, H. Brinkschulte, J. Jacquinot, K. D. Lawson, A. Kaye, and J. A. Tagle, Plasma Phys. Contr. Fusion **30**, 149 (1988).

[3] J. Tachon, in *Physics of Plasma–Wall Interactions in Controlled Fusion*, edited by D. E. Post and R. Behrisch (Plenum, New York, 1986), pp. 1005–1066.

[4] J. B. O. Caughman, II, D. N. Ruzic, and D. J. Hoffman, J. Vac. Sci. Technol. A **5**, 2301 (1987).

[5] B. Stratton, H. W. Moos, W. L. Hodge, S. Suckewer, J. C. Hosea, R. A. Hulse, D. Q. Hwang, and J. R. Wilson, Nucl. Fusion **24**, 767 (1984).

[6] J.-M. Noterdaeme, G. Janeschitz, K. McCormick, J. Neuhauser, J. Roth, F. Ryter, E. Taglauer, N. Tsois *et al.*, in *Proceedings of the 14th European Conference on Controlled Fusion and Plasma Heating, Madrid, 1987*, edited by F. Engelmann and J. L. Alvarez Rivas (European Physical Society, 1987), Vol. II, p. 678.

[7]H. Ogawa, K. Odajima, H. Ohtsuka, H. Matsumoto, and H. Kimura *et al.*, J. Nucl. Mater. **128/129**, 298 (1984).
[8]R. Behrisch, F. Wesner, M. Wielunski, J.-M. Noterdaeme, and E. Taglauer, in Ref. 6, p. 778.
[9]S. Puri, in *Proceedings of the 15th European Conference on Controlled Fusion and Plasma Heating*, Dubrovnik, 1988, edited by S. Pesic and J. Jacquinot (European Physical Society, 1988), Vol. II, p. 754.
[10]W. Gardner, T. S. Bigelow, G. R. Haste, D. J. Hoffman, R. L. Livesey, and D. R. Roberts, Bull. Am. Phys. Soc. **31**, 1418 (1986).
[11]N. Benjamin, Rev. Sci. Instrum. **53**, 1541 (1982).
[12]J. A. Schmidt, Rev. Sci. Instrum. **39**, 1297 (1968).
[13]F. F. Chen, in *Plasma Diagnostic Techniques*, edited by R. H. Huddlestone and S. L. Leonard (Academic, New York, 1965), p. 196.
[14]N. Hershkowitz, M. H. Cho, C. H. Nam, and T. Intrator, Plasma Chem. Plasma Proc. **8**, 35 (1988).
[15]A. Boschi and F. Magistrelli, Nuovo Cimento **29**(2), 487 (1963).
[16]J. S. deGrassie, J. C. DeBoo, M. A. Mahdavi, N. Ohyabu, and M. Shimada, J. Vac. Sci. Technol. **20**, 1222 (1982).
[17]I. S. Lehrman, P. L. Colestock, G. J. Greene, D. H. McNeil, M. Ono, J. R. Wilson, D. M. Manos, S. Bernabei, and J. L. Shohet, in *Proceedings of the Seventh Topical Conference on Applications of Radio-Frequency Power to Plasmas*, edited by S. Bernabei and R. W. Motley (AIP, New York, 1987), pp. 274–277.
[18]D. N. Ruzic, D. Heifetz, and S. A. Cohen, J. Nucl. Mater. **145/146**, 527 (1987).
[19]P. C. Stangeby, Phys. Fluids **27**, 682 (1984).
[20]E. Y. Wang, N. Hershkowitz, D. Diebold, T. Intrator, R. Majeski *et al.*, J. Appl. Phys. **61**, 4786 (1987).
[21]R. Chodura, Phys. Fluids **25**, 1628 (1982).
[22]A. B. Dewald, A. W. Bailey, and J. N. Brooks, Phys. Fluids **30**, 267 (1987).
[23]J. L. Wilson, J. B. O. Caughman, II, Phi Long Nguyen, and D. N. Ruzic, J. Vac. Sci. Technol. A **7**, 972 (1989).
[24]J. B. O. Caughman, II, D. N. Ruzic, and D. J. Hoffman, Bull. Am. Phys. Soc. **33**, 2017 (1988).
[25]J. Roth, J. Bohdansky, and W. Ottenberger, IPP Report No. 9/26, 1979, Max-Planck-Institut für Plasmaphysik, D-8046 Garching bei München.